

Raman Spectroscopy Study on CsB₃O₅ Crystal–Melt Boundary Layer Structure

Songming Wan,^{*,†} Xia Zhang,[†] Sijie Zhao,[‡] Qingli Zhang,[†] Jinglin You,[‡] Lu Lu,[§] Peizhen Fu,[§] Yicheng Wu,[§] and Shaotang Yin[†]

Anhui Institute of Optics and Fine Mechanics, Chinese Academy of Sciences, Hefei 230031, China, School of Material Science and Engineering, Shanghai University, Shanghai 200072, China, and Technical Institute of Physics and Chemistry, Chinese Academy of Sciences, Beijing 100080, China

Received October 19, 2006; Revised Manuscript Received October 6, 2007

ABSTRACT: The structure of the melt near a crystal–melt interface is a fundamental problem in the dynamics of crystal growth. In this work, high-temperature Raman spectroscopy was used to investigate the melt structure near the CsB₃O₅ (CBO) crystal–melt interface. An ordered boundary layer was observed near the interface; its thickness is larger than 100 μm . An isomerization reaction between 3- and 4-coordinated boron was found in the layer. The ordering of the melt is strongest near the crystal–melt interface and decreases toward the bulk melt. These results have been applied to explain the growth habit of CBO crystal. The predicted growth habit is in good agreement with the observed result.

1. Introduction

The structure of the melt near a crystal–melt interface is a fundamental problem in the dynamics of crystal growth because of its importance in understanding a variety of crystal growth phenomena including the habit of crystal growth, incorporation of impurities, and dendritic growth.¹ Various theoretical and numerical studies have been performed in order to investigate the structure. Molecular dynamic (MD) and Monte Carlo (MC) simulation showed that, at a crystal–melt interface, the well-ordered crystal surface induces the melt ordering in its vicinity, and a transition layer with several molecular layers exists between the fully ordered crystal and the fully disordered melt² (In this paper, we call the transition layer the crystal–melt boundary layer.). However, direct experimental studies of the boundary layer structure at the molecular level are sparse so far. Recently, HPCIM (holographic phase contrast interferometric microphotograph) and Raman spectroscopy techniques have been applied to study the crystal–solution boundary layer structure of a growing KH₂PO₄ (KOP) crystal.³ The results showed that its boundary layer thickness is larger than 100 μm . In the layer, the solute concentration sharply varies from the crystal surface to its bulk solution. More interesting, some significant characteristics of the ploy-phase reactions relating to KDP crystal growth occur in the layer. These experimental results imply that the structure of the crystal–melt boundary layer may be more complicated than has been assumed.

CsB₃O₅ (CBO) crystal is an important nonlinear optical crystal for frequency conversion in the ultraviolet region.⁴ In this paper, we select the CBO crystal–melt system to study its boundary layer structure in virtue of the following reasons: (1) The triborate group ([B₃O₇], O = bridging oxygen atom, consisting of two three-coordinated B₃O₃ units and one four-coordinated B₄O₄ unit, as shown in the Supporting Information) is the only structural group forming the CBO crystal structure.⁵ (2) The structure of various borate groups in binary alkali borate crystals/melts has been studied through Raman spectroscopy.

(3) CBO crystal melts congruently at a relative low temperature (835 °C), which is convenient for us to make a CBO crystal–melt equilibrium system in a crystal growth cell.

Compared with other analysis techniques, high-temperature Raman spectroscopy combines the advantages of in situ observation, microscale analysis, and high-temperature measurement and is widely used to investigate the structure of crystals/melts. In this paper, high-temperature Raman spectroscopy was applied to study in situ the structure of the melt near the CBO crystal–melt interface; then, the growth habit of CBO crystal was predicted. Our work proves that high-temperature Raman spectroscopy is a powerful tool to study the mechanism of a crystal growing from its high-temperature melt and numerous related dynamic phenomena.

2. Experimental Section

Our experimental system comprises two components: a high-temperature Raman spectrometer and a crystal growth cell (see Figure 1). Unpolarized Raman spectra were recorded by the commercial spectrometer (Jobin Yvon U1000) with a back scattering configuration. An ICCD (intensive charge couple device) was employed as the detector. The excitation source was the 532 nm line of a Q-switch pulsed SHG-Nd:YAG laser. The spectra of the crystal samples were collected by accumulating 30 scans; each scan time was 6 s. The scan number for melt samples was 5 times in order to avoid the laser-induced heat damaging the melt structure. The spectral resolution was 2 cm^{-1} . The growth cell was fabricated from high-grade stainless steel and consists of a water jacket surrounding the main sample chamber. A platinum boat of dimensions 5 × 10 × 20 mm is placed in the center of the chamber and heated on the right side by a platinum wire winding. The heating system provides a horizontal temperature gradient in the boat.

The CBO single crystal used for this study was grown from a stoichiometric melt. The single crystal was cut into slices slightly smaller than the platinum boat. One such slice was then mounted in the platinum boat. By carefully controlling the temperature, a steady crystal–melt interface was produced. After that, the laser beam was focused on different positions near the crystal–melt interface to study the microstructure of the crystal/melt (the positions are shown in Figure 2).

3. Results and Discussion

CBO crystal was found in 1957. It has orthorhombic structure with a space group of $P2_12_12_1$. The structure of CBO crystal only contains Cs cations and triborate groups which form a

* Corresponding author. E-mail: smwan@aiofm.ac.cn. Tel.: +86-0551-5591039. Fax: +86-0551-5591039.

[†] Anhui Institute of Optics and Fine Mechanics.

[‡] Shanghai University.

[§] Technical Institute of Physics and Chemistry.

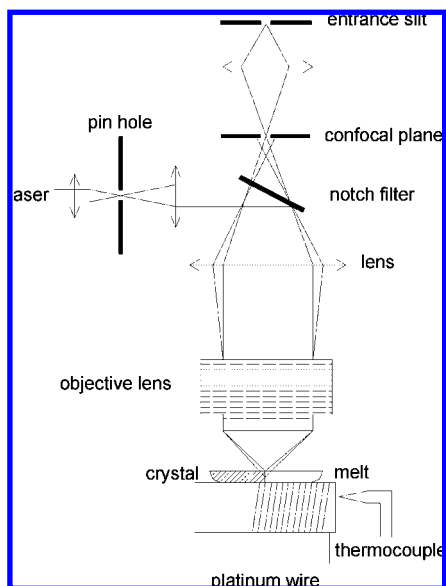


Figure 1. Schematic diagram of the experimental system for Raman spectroscopic measurement.

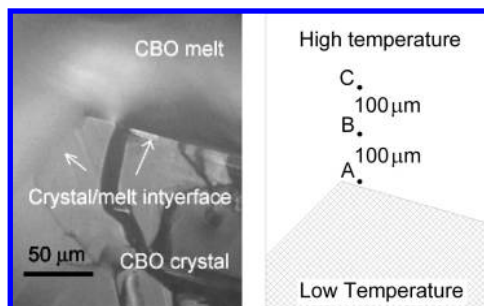


Figure 2. Typical CBO crystal–melt interface with the measurement positions. Positions A, B, and C are in the melt 5, 100, and 200 μm from the interface, respectively.

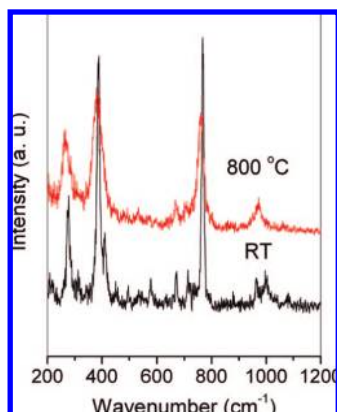


Figure 3. Raman spectra of CBO crystal at room temperature (bottom) and 800 $^{\circ}\text{C}$ (top).

three-dimensional boron–oxygen network.⁵ (see the Supporting Information) Therefore, most of the Raman bands of CBO crystal can be assigned to the characteristic vibrational modes of the triborate group. The Raman spectrum of CBO crystal at room temperature is presented in Figure 3. The assignment of the vibrational bands can be found in the literature.⁶ In order to study the Raman spectra of the CBO melt, the Raman spectra of CBO crystal at high temperatures were recorded, a typical

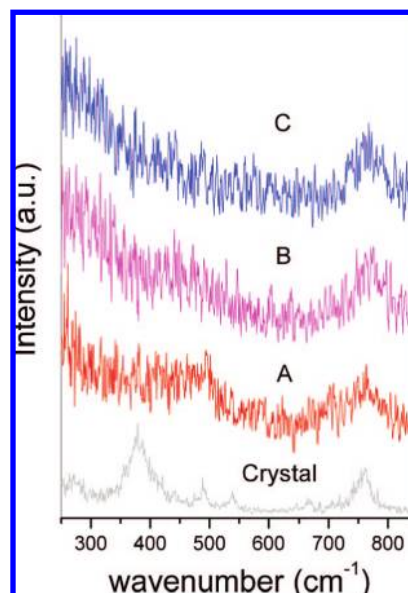


Figure 4. Raman spectra of positions A, B, C, and CBO crystal near the crystal–melt interface. Positions A, B, and C are in the melt 5, 100, and 200 μm from the interface, respectively.

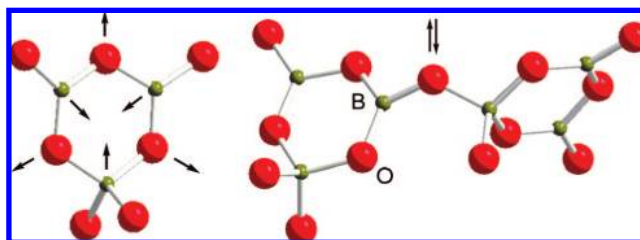


Figure 5. Schematic representations of the atom motions of the vibrational bands at 760 cm^{-1} (left) and 400–500 cm^{-1} (right).

Raman spectrum (at 800 $^{\circ}\text{C}$) is shown in Figure 3. With the temperature increasing, all of the peaks broaden and decrease in frequency due to the wider bond angle distribution and the increases in interatomic distances at higher temperatures.

Figure 4 shows the Raman spectrum of CBO crystal at the temperature just below its melting point and the Raman spectra of the CBO melt near the crystal–melt interface (The measurement positions are shown in Figure 2.). With the melting of the crystal, the Raman spectra changed dramatically because the periodic crystal structure was destroyed. Two bands which respectively were located at around 760 cm^{-1} and in the range of 400–500 cm^{-1} appear in the Raman spectra of the melt. Both of them are the characteristic vibrational bands of triborate group. The strongest band around 760 cm^{-1} was assigned by Brill to the symmetric breathing vibration of boroxol rings, where the π -band character in the rings is disturbed, such as the rings with one or two BO_4 tetrahedra (see Figure 5) and the rings with one or two nonbridging oxygen atoms.⁷ The band in the range of 400–500 cm^{-1} was assigned by Kamitsos et al. to the symmetric or antisymmetric stretching vibration of BO_4 tetrahedra in the triborate groups.⁸ Galeener et al. also suggested that the band (near 470 cm^{-1}) is associated with the symmetric stretching vibration of the oxygen atom that bridges two boroxol rings (see Figure 5).⁹ When the laser beam moved from position A to B, the band at around 500 cm^{-1} shifted to around 450 cm^{-1} as a result of the increase in the interatomic distance of the B–O–B bridge bond between two boroxol rings. At position C, the 760 cm^{-1} band remains, indicating that the boroxol rings

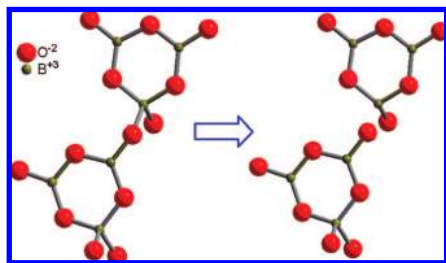


Figure 6. Schematic illustration of the isomerization reaction occurring in the boundary layer.

exist in that position. On the other hand, the 450 cm^{-1} band vanishes, indicating that a process involving the break and reform related to the BO_4 tetrahedra took place in the position. Yiannopoulos et al. have found that an isomerization reaction between 3- and 4-coordinated boron occurred in $\text{Na}_2\text{O}-\text{B}_2\text{O}_3$ and $\text{K}_2\text{O}-\text{B}_2\text{O}_3$ melts at high temperature: One $\text{B}-\text{O}$ bond of BO_4 tetrahedron breaks, and then, one $\text{B}\text{O}_2\text{O}$ unit consisting of two bridging oxygens and one nonbridging oxygen is generated.¹⁰ The result is consistent with our experimental result in the CBO melt. Further, we propose a structural rearrangement model for the isomerization reaction occurring in the CBO crystal–melt boundary layer, as shown in Figure 6.

The above experimental results also show that a preordering boundary layer is formed near the crystal–melt interface when CBO crystal is in equilibrium with its melt. Its thickness is larger than $100\ \mu\text{m}$ (the distance between position B and the interface). These experimental results are compatible with the model that assumes a mesophase layer present in front of a growing crystal; the crystal does not grow into the bulk melt, but into the mesophase.¹¹

The growth habit of CBO crystal can be explained based on the above results. In general, the shape of a crystal is determined by the relative rates of deposition of crystal growth units on its various faces; faces that grow slower appear as larger developed faces. Further, the growth rates are determined primarily by the strength of binding between the growth units and the crystal surfaces. The slowest growing, and hence the largest faces, are those with the weakest strength of binding.¹² From the above experimental results, we know that the weakest bond in the triborate group is the $\text{B}-\text{O}-\text{B}$ bridge bond between two triborate groups. Thus, the faces only containing BO_4 tetrahedra possess the weakest strength of binding. According to the structure of CBO crystal, the faces only containing BO_4 tetrahedra are parallel to (101) , $(\bar{1}01)$, $(10\bar{1})$, $(\bar{1}0\bar{1})$, (011) , $(0\bar{1}\bar{1})$, $(01\bar{1})$, and $(0\bar{1}1)$ faces; therefore, these faces should be the larger developed faces. The case of the (011) face is shown in Figure 7. The morphology of CBO crystal has been studied by Chang et al.,¹³ and the observed growth habit is in good agreement with our predicted result.

4. Conclusion

High-temperature Raman spectroscopy has been used to investigate the boundary layer structure of the CBO crystal–melt system. An ordered boundary layer was observed near the CBO crystal–melt interface; its thickness is larger than $100\ \mu\text{m}$. An isomerization reaction between 3- and 4-coordinated boron was found in the layer. The ordering of the melt is strongest near the crystal–melt interface and decreases toward the bulk melt. These results have been applied to explain the growth habit of CBO crystal, and the predicted growth habit is in good agreement with the observed result.

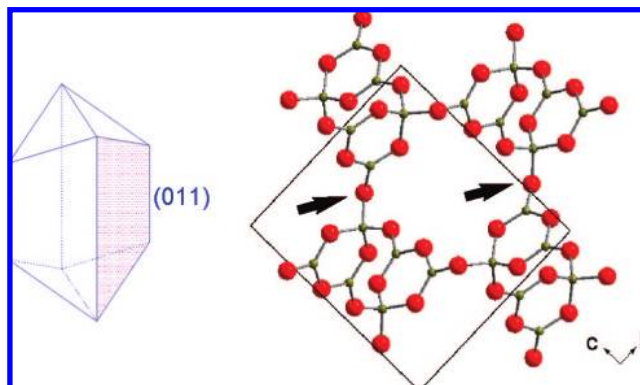


Figure 7. Morphology of CBO crystal growing from its melt (left) and the packing arrangement of CBO crystal as viewed along the a axis (right). The bridging oxygen atoms between the two triborate groups are indicated by the arrows.

Currently, the great demand for high-quality crystals has provided practical incentives to study the dynamics of crystal growth and many related problems. Crystal–melt boundary layer structure is an important aspect for the deeper understanding of these problems. Our work has demonstrated that high-temperature Raman spectroscopy is a powerful tool to study the structure of a crystal–melt boundary layer on the atomic scale. We believe that this technique has the potential to enhance our knowledge of numerous processes involved in crystal growth.

Acknowledgment. This work is financially supported by the National Natural Science Foundation of China (Grant Nos. 50472104 and 60378026). The authors are also grateful to Dr. Huaili Qiu and Prof. Aihua Wang for constructing the in situ crystal growth cell, and Ms. Li Huang for technical support and helpful discussion.

Supporting Information Available: Triborate groups in the CBO crystal structure (PDF). This material is available free of charge via the Internet at <http://pubs.acs.org>.

References

- (1) Chernov, A. A. *J. Cryst. Growth* **2004**, *264*, 499–518.
- (2) (a) Davidchack, R. L.; Laird, B. B. *J. Chem. Phys.* **1998**, *108*, 9452–9462. (b) Bonissent, A.; Gauthier, E.; Finney, J. L. *Philos. Mag. B* **1979**, *39*, 49. (c) Curtin, W. A. *Phys. Rev. Lett.* **1987**, *59* (11), 1228–1231.
- (3) Yu, X. L.; You, J. L.; Wang, Y.; Cheng, Z. X.; Yu, B. K.; Zhang, S. J.; Sun, D. L.; Jiang, G. C. *Sci. Chin. E* **2001**, *44* (3), 265–273.
- (4) Wu, Y. C.; Fu, P. Z.; Wang, J. X.; Xu, Z. Y.; Zhang, L.; Kong, Y. F.; Chen, C. T. *Opt. Lett.* **1997**, *22*, 1840–1842.
- (5) Krogh-Moe, J. *Ark. Kemi* **1958**, *12*, 247.
- (6) Wang, Y. F.; Liu, J. J.; Hu, S. F.; Lan, G. X.; Fu, P. Z.; Wang, J. X. *J. Raman Spectrosc.* **1999**, *30*, 519–523.
- (7) Brill, T. W. *Philips. Res. Rep. Suppl.* **1976**, *2*, 1–107.
- (8) Kamitsos, E. I.; Karakasside, M. A. *Phys. Chem. Glasses* **1989**, *30* (1), 19–26.
- (9) Galeener, F. L.; Thorpe, M. F. *Phys. Rev. B* **1983**, *28* (15), 5802–5813.
- (10) (a) Akagi, R.; Ohtori, N.; Umesaki, N. *J. Non-Cryst. Solid* **2001**, *293–295*, 471–476. (b) Yiannopoulos, Y. D.; Kamitsos, E. I.; Chryssikos, J. A. In *Proceedings of the Second International Conference on Borate Glasses/1996*; Wright, A. C., Feller, S. A., Hannon, A. C., Eds.; Alden: Oxford, 1997; p 514. (c) Chryssikos, G. D.; Kamitsos, E. I.; Karakasside, M. A. *Phys. Chem. Glasses* **1990**, *31* (3), 109–116.
- (11) Bilgram, J. H.; Steininger, R. *J. Cryst. Growth* **1990**, *99*, 30–37.
- (12) Berkovitch-Yellin, Z. *J. Am. Chem. Soc.* **1985**, *107*, 8239–8253.
- (13) Chang, F.; Fu, P. Z.; Wu, Y. C.; Chen, G. J.; Xu, Z. J.; Chen, C. T. *J. Cryst. Growth* **2005**, *277*, 298–302.